

No.39

AUGUST 2004.

CONTENTS

	pg.
The Flores Knots	903

A quarterly publication
for
the braiding artisan

Resale of this publication or copies thereof
is strictly prohibited

Copyright ©2004 by :

{ A.G. Schaake; 21 Sundown Cresc.; Hamilton; New Zealand.
D. Van Tassel; Box 335; Craig, Co 81626-0335; U.S.A.
F.J.M. Masurel; Ganzenzijde 4; 2317 XG Leiden; Nederland.

All rights reserved. No part of this publication may be reproduced, stored in a retrieval system, or transmitted, in any form or by any means, electronic, mechanical, photo-copying, recording, or otherwise, without prior written permission.

This publication is available to braiding artisans only.

Copies may be obtained from :

A.G. Schaake,
21 Sundown Cresc.,
Hamilton,
New Zealand.

The Flores Knots

In the *Encyclopedia of Rawhide and Leather Braiding* on pg. 424 Bruce Grant writes the following:

This beautiful little button [the Flores Button Knot] was shown to me in November 1966, in Buenos Aires by my amigo, Don Luis Alberto Flores. It illustrates a unique way to make a herringbone weave on a five-part, six-bight Turk's-head — or armadura, as they say in the Argentine.

From the above statement it is quite clear that it was not realised what in fact this knot was all about. Furthermore, from the three coding errors it contains, it appears that the knot was an empirical discovery (see later). The Flores Button Knot described by Bruce in the *Encyclopedia* is a single-string imitation of its true two-string characteristic, and since this single-string imitation of a true two-string characteristic is the usual encountered one, it contains a noticeable irregularity. Hence let's first have a look at this single-string imitation.

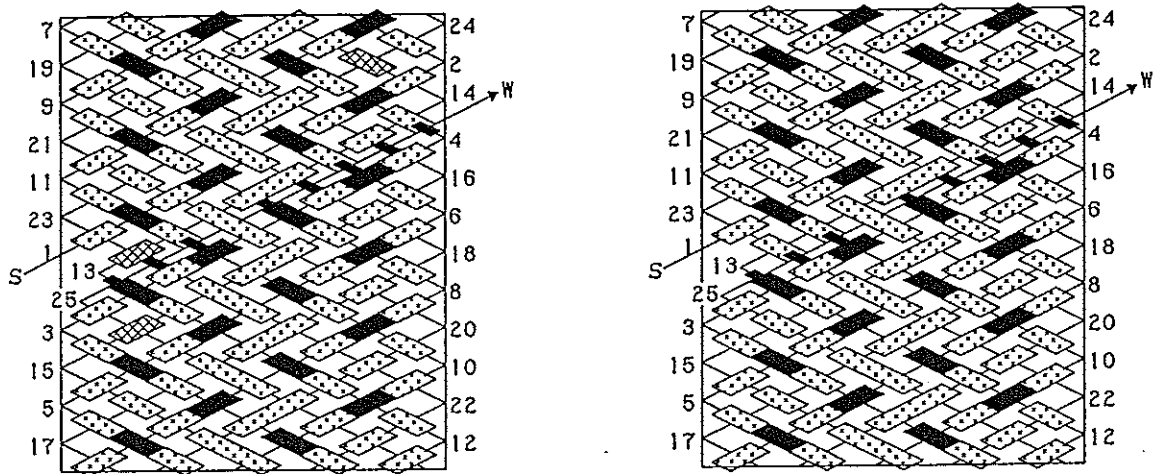


Fig. 714 — The Flores Button Knot.

The left-hand grid-diagram in Fig. 714 depicts the Flores Button Knot described by Bruce Grant. Its half-cycle braiding algorithms are as follows:

- | | |
|-----------------------|----------------------|
| 1. Free run. | 13. $u - o - 2u$. |
| 2. Free run. | 14. $2u - o - 2u$. |
| 3. Free run. | 15. $2u - o - 2u$. |
| 4. u . | 16. $3u - o - 2u$. |
| 5. u . | 17. $3u - o - 2u$. |
| 6. $u - o$. | 18. $4u - o - 2u$. |
| 7. $u - o$. | 19. $4u - o - 2u$. |
| 8. $u - o - u$. | 20. $4u - 2o - 2u$. |
| 9. $u - o - u$. | 21. $4u - 2o - 2u$. |
| 10. $u - o - u - o$. | 22. $4u - 2o - 3u$. |
| 11. $u - o - u - o$. | 23. $4u - 2o - 3u$. |
| 12. $u - o - u - o$. | 24. $4u - 2o - 3u$. |
| | 25. $9u$. |

Note that Bruce Grant does not work in exact half-cycles; however, it is important to work in exact half-cycles only. It is readily observed from the grid-diagram that three crossing-points are coded incorrectly: to be consistent the second and the eighth column

from the left should be column-coded. The correct coding for this knot is shown by the right-hand grid-diagram of Fig. 714; its half-cycle braiding algorithms are as follows:

- | | |
|----------------------|----------------------------|
| 1. Free run. | 13. $u - o - 2u.$ |
| 2. Free run. | 14. $2u - o - 2u.$ |
| 3. Free run. | 15. $2u - o - 2u.$ |
| 4. $u.$ | 16. $3u - o - 2u.$ |
| 5. $u.$ | 17. $3u - o - 2u.$ |
| 6. $u - o.$ | 18. $4u - o - 2u.$ |
| 7. $u - o.$ | 19. $4u - o - 2u.$ |
| 8. $u - o - u.$ | 20. $4u - 2o - 2u.$ |
| 9. $u - o - u.$ | 21. $4u - 2o - 2u.$ |
| 10. $u - o - u - o.$ | 22. $4u - 2o - u - o - u.$ |
| 11. $u - o - u - o.$ | 23. $4u - 2o - u - o - u.$ |
| 12. $u - o - u - o.$ | 24. $4u - 2o - u - o - u.$ |
| | 25. $9u.$ |

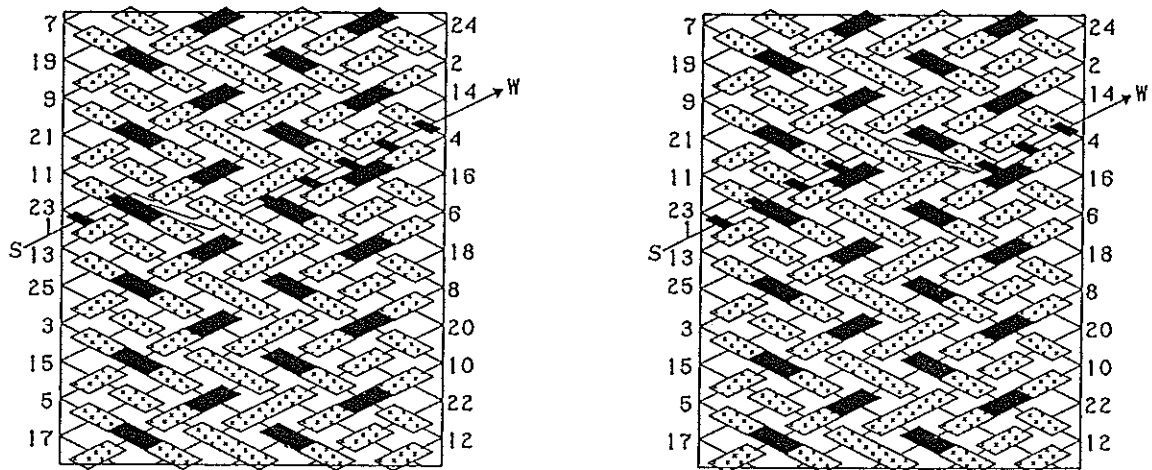


Fig. 715 — The Flores Knot without the boundary irregularity.

The already mentioned irregularity in the braid can be avoided by braiding the knot as shown by the grid-diagrams in Fig. 715 for example. The half-cycle braiding algorithms associated with the left-hand grid-diagram in Fig. 715 are as follows:

- | | |
|----------------------|----------------------------|
| 1. Free run. | 13. $u - o - 2u.$ |
| 2. Free run. | 14. $2u - o - 2u.$ |
| 3. Free run. | 15. $2u - o - 2u.$ |
| 4. $u.$ | 16. $3u - o - 2u.$ |
| 5. $u.$ | 17. $3u - o - 2u.$ |
| 6. $u - o.$ | 18. $4u - o - 2u.$ |
| 7. $u - o.$ | 19. $4u - o - 2u.$ |
| 8. $u - o - u.$ | 20. $4u - 2o - 2u.$ |
| 9. $u - o - u.$ | 21. $4u - 2o - 2u.$ |
| 10. $u - o - u - o.$ | 22. $4u - 2o - 2u - o.$ |
| 11. $u - o - u - o.$ | 23. $4u - 2o - u - o - u.$ |
| 12. $u - o - u - o.$ | 24. $4u - 2o - u - o - u.$ |
| | 25. $9u.$ |

The half-cycle braiding algorithms associated with the right-hand grid-diagram in Fig. 715 are as follows:

- | | |
|-----------------------|-----------------------------|
| 1. Free run. | 13. $u - o - 2u$. |
| 2. Free run. | 14. $2u - o - 2u$. |
| 3. Free run. | 15. $2u - o - 2u$. |
| 4. u . | 16. $3u - o - 2u$. |
| 5. u . | 17. $3u - o - 2u$. |
| 6. $u - o$. | 18. $3u - 2o - 2u$. |
| 7. $u - o$. | 19. $4u - o - 2u$. |
| 8. $u - o - u$. | 20. $4u - o - u - o - u$. |
| 9. $u - o - u$. | 21. $4u - 2o - 2u$. |
| 10. $u - o - u - o$. | 22. $4u - 2o - 2u - o$. |
| 11. $u - o - u - o$. | 23. $4u - 2o - u - o - u$. |
| 12. $u - o - u - o$. | 24. $4u - 2o - u - o - u$. |
| | 25. $4u - 2o - 3u$. |

These knots are single-string imitations of the true two-string form, hence let's call the true two-string form the Flores Knot. But what is the Flores Knot then really and what is its physical appearance?

The physical appearance of the Flores Knot is that of the Semi-Standard Herringbone Pineapple Knot with $A = 2, x = 6, B^* = 6$ (see the left-hand grid-diagram of Fig. 716).

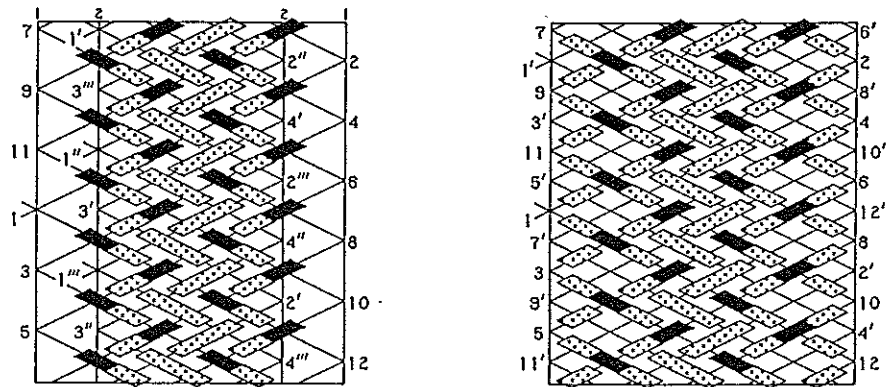


Fig. 716 — The evolution of the Flores Knot from the Semi-Standard Herringbone Pineapple Knot.

The right-hand grid-diagram in Fig. 716 shows how the Flores Knot evolves from it while retaining the physical appearance of the Semi-Standard Herringbone Pineapple knot from which it evolves. In this right-hand grid-diagram there are crossings in the second and penultimate crossing-columns which do not yet have a superimposed coding. Note that the codings of those crossings do not affect the physical appearance of the knot. Although each of those crossings can therefore be given an arbitrary coding, we limit these codings so that:

1. The columns to which they belong become column-coded.
2. The rows to which they belong become row-coded.

When we fulfil the column-coding option (option 1. above), then the Flores Knot is depicted by the left-hand grid-diagram in Fig. 717. The Flores Knot is an interbraid of an over-under coded Regular Knot and a two-pass Spanish Ring Knot.

When we fulfil the row-coding option (option 2. above), then the Flores Knot is depicted by the left-hand grid-diagram in Fig. 718. The Flores Knot is an interbraid of two over-under coded Regular Knots.

Note that the Flores knot requires two essential strings, whereas the Semi-Standard Herringbone Pineapple knot from which it has evolved, but to which it is identical in physical appearance, requires four essential strings.

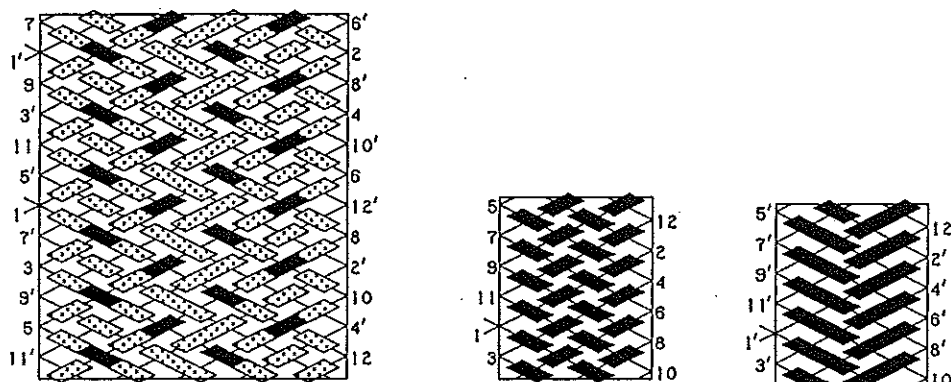


Fig. 717 — The Column-coding option.

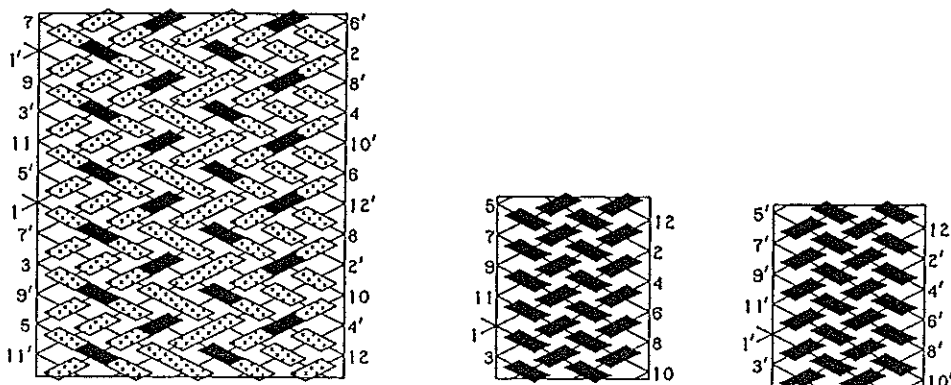


Fig. 718 — The Row-coding option.

★★ Draw for each of the left-hand grid-diagrams in Figs. 717 & 718 the path in the RKT and from it determine their Δ^* values, then construct their algorithm diagrams. Read from their algorithm diagrams their half-cycle braiding algorithms.

There is of course no reason why a Flores Knot should be restricted in having to be evolved in the above discussed manner from a two-pass Semi-Standard Herringbone Pineapple Knot. It can as well evolve in a similar manner from an *A*-pass Herringbone Pineapple Knot in general.

From the Standard and Semi-Standard Herringbone Pineapple Knots to the Flores Knots.

In Fig. 719 are depicted the string-runs of two Flores Knot examples: the upper diagram depicts the evolution of the string-run of a Flores Knot from the string-run of a six-pass Standard Herringbone Pineapple Knot, and the lower diagram depicts the evolution of the string-run of a Flores Knot from the string-run of a five-pass Semi-Standard Herringbone Pineapple Knot.

Since *A*-pass Standard and Semi-Standard Herringbone Pineapple Knots consist of *A* components (their string-run is such that $\left| \frac{x}{2} - (1 + r_1) \right|_A = \left| \frac{x}{2} - (1 + k) \right|_A = \frac{A}{2}$, hence $y = A$), the Flores Knots evolved from them also consist of *A* components.†

† Refer to *The Braider*, Issue No. 23, pp. 513-515, 526 and Issue No. 24, pg. 557.

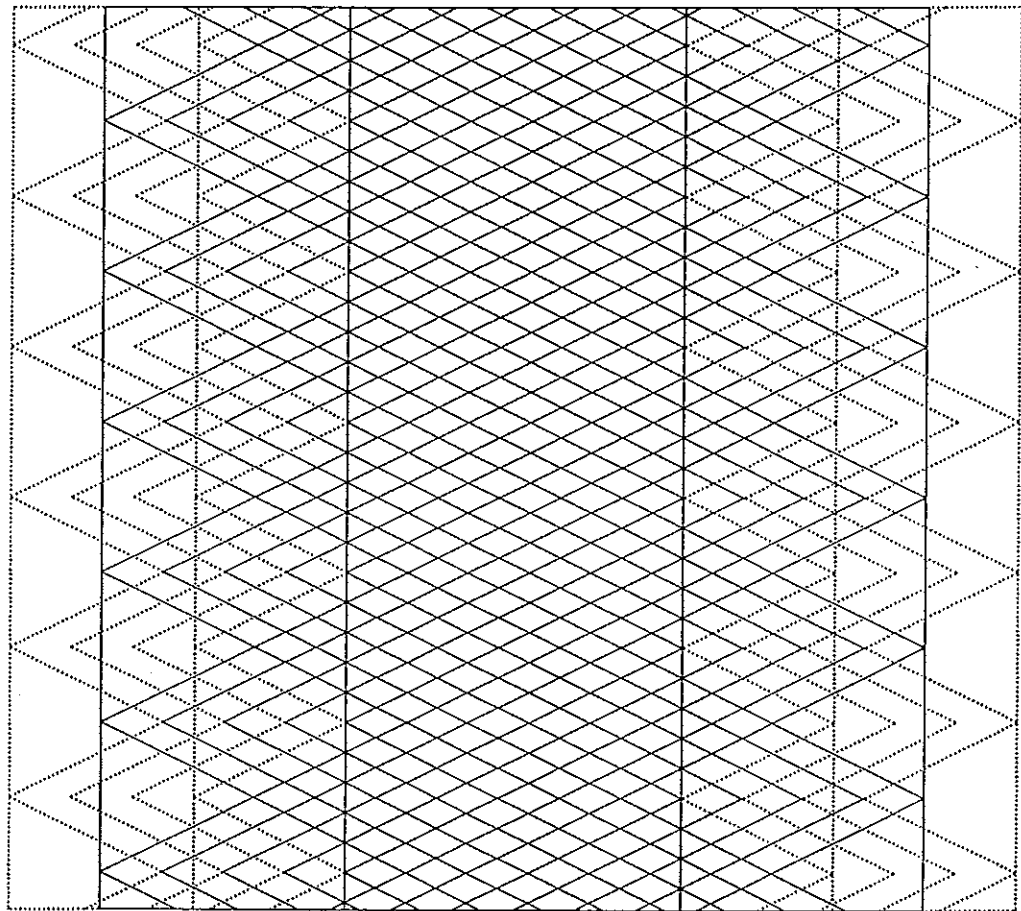
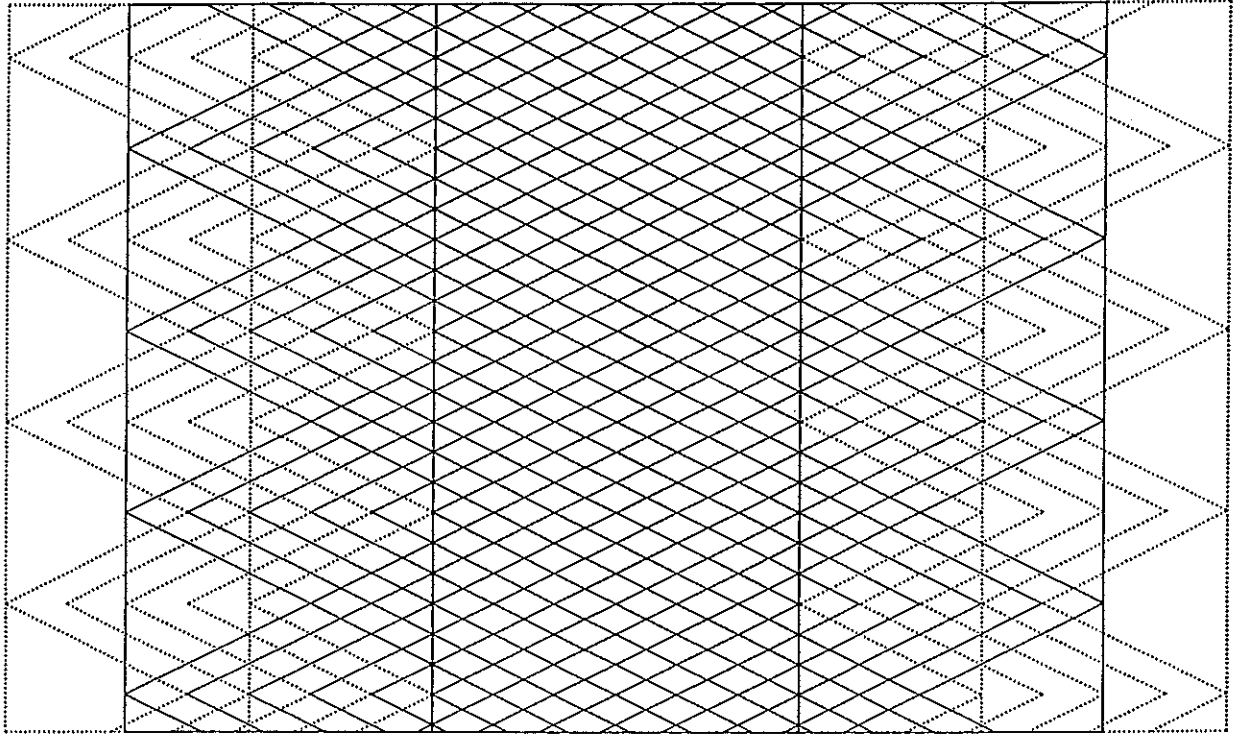


Fig. 719 — Flores Knot string-runs evolved from Standard or Semi-Standard Herringbone Pineapple Knot string-runs.

Let the number of parts of the Standard or Semi-Standard Herringbone Pineapple Knot component with the lower-left to upper-right half-cycle $l_i \rightarrow r_i$ be P_{cP} and let the number of parts of its associated Flores knot component be P_{cF} , then the following relationships apply:

- i). For $l_i = 1$ and $r_i = 1$: $P_{cF} = P_{cP}$.
- ii). For $l_i = 1$ and $1 < r_i \leq A$: $P_{cF} = P_{cP} + 1$.
- iii). For $1 < l_i \leq A$ and $r_i = 1$: $P_{cF} = P_{cP} + 1$.
- v). For $1 < l_i \leq A$ and $1 < r_i \leq A$: $P_{cF} = P_{cP} + 2$.

Example 1.

Herringbone Pineapple Knot with $A = 6$; $x = 12$; $k = \left\lfloor \frac{x+A}{2} - 1 \right\rfloor_A = 2$; $B^* = 4$.

Its string-run is contained in the upper diagram of Fig. 719.

For $l_i = 1$; $r_i = k = 2$: $P_{cP} = 4 + \frac{x-2(k+1)}{A} = 5$.[†] Hence $P_{cF} = P_{cP} + 1 = 5 + 1 = 6$ for the associated Flores Knot component. The number of essential strings for the associated Flores component is thus $\text{g.c.d.}(P_{cF}, B^*) = \text{g.c.d.}(6, 4) = 2$.

For $l_i = 2$; $r_i = 1$: $P_{cP} = 4 + \frac{x-2(k+1)}{A} = 5$. Hence $P_{cF} = P_{cP} + 1 = 5 + 1 = 6$ for the associated Flores Knot component. The number of essential strings for the associated Flores component is thus $\text{g.c.d.}(P_{cF}, B^*) = \text{g.c.d.}(6, 4) = 2$.

For $l_i = 3$; $r_i = A = 6$: $P_{cP} = 2 + \frac{x-2(k+1)}{A} = 3$.[‡] Hence $P_{cF} = P_{cP} + 2 = 3 + 2 = 5$ for the associated Flores Knot component. The number of essential strings for the associated Flores component is thus $\text{g.c.d.}(P_{cF}, B^*) = \text{g.c.d.}(5, 4) = 1$.

For $l_i = 4$; $r_i = 5$: $P_{cP} = 2 + \frac{x-2(k+1)}{A} = 3$. Hence $P_{cF} = P_{cP} + 2 = 3 + 2 = 5$ for the associated Flores Knot component. The number of essential strings for the associated Flores component is thus $\text{g.c.d.}(P_{cF}, B^*) = \text{g.c.d.}(5, 4) = 1$.

For $l_i = 5$; $r_i = 4$: $P_{cP} = 2 + \frac{x-2(k+1)}{A} = 3$. Hence $P_{cF} = P_{cP} + 2 = 3 + 2 = 5$ for the associated Flores Knot component. The number of essential strings for the associated Flores component is thus $\text{g.c.d.}(P_{cF}, B^*) = \text{g.c.d.}(5, 4) = 1$.

For $l_i = 6$; $r_i = 3$: $P_{cP} = 2 + \frac{x-2(k+1)}{A} = 3$. Hence $P_{cF} = P_{cP} + 2 = 3 + 2 = 5$ for the associated Flores Knot component. The number of essential strings for the associated Flores component is thus $\text{g.c.d.}(P_{cF}, B^*) = \text{g.c.d.}(5, 4) = 1$.

Hence the total number of essential strings for the Flores Knot is 8, whereas the Herringbone Pineapple knot required 6 essential strings.

Example 2.

Herringbone Pineapple Knot with $A = 5$; $x = 11$; $k = \left\lfloor \frac{x+A}{2} - 1 \right\rfloor_A = 2$; $B^* = 6$.

Its string-run is contained in the lower diagram of Fig. 719.

For $l_i = 1$; $r_i = k = 2$: $P_{cP} = 4 + \frac{x-2(k+1)}{A} = 5$. Hence $P_{cF} = P_{cP} + 1 = 5 + 1 = 6$ for the associated Flores Knot component. The number of essential strings for the associated Flores component is thus $\text{g.c.d.}(P_{cF}, B^*) = \text{g.c.d.}(6, 6) = 6$.

For $l_i = 2$; $r_i = 1$: $P_{cP} = 4 + \frac{x-2(k+1)}{A} = 5$. Hence $P_{cF} = P_{cP} + 1 = 5 + 1 = 6$ for the associated Flores Knot component. The number of essential strings for the associated Flores component is thus $\text{g.c.d.}(P_{cF}, B^*) = \text{g.c.d.}(6, 6) = 6$.

[†] Refer to *The Braider*, Issue No. 23, pg. 521.

[‡] Refer to *The Braider*, Issue No. 23, pg. 521.

For $l_i = 3 ; r_i = A = 5 : P_{cP} = 2 + \frac{x-2(k+1)}{A} = 3$. Hence $P_{cF} = P_{cP} + 2 = 3 + 2 = 5$ for the associated Flores Knot component. The number of essential strings for the associated Flores component is thus $\text{g.c.d.}(P_{cF}, B^*) = \text{g.c.d.}(5, 6) = 1$.

For $l_i = 4 ; r_i = 4 : P_{cP} = 2 + \frac{x-2(k+1)}{A} = 3$. Hence $P_{cF} = P_{cP} + 2 = 3 + 2 = 5$ for the associated Flores Knot component. The number of essential strings for the associated Flores component is thus $\text{g.c.d.}(P_{cF}, B^*) = \text{g.c.d.}(5, 6) = 1$.

For $l_i = 5 ; r_i = 3 : P_{cP} = 2 + \frac{x-2(k+1)}{A} = 3$. Hence $P_{cF} = P_{cP} + 2 = 3 + 2 = 5$ for the associated Flores Knot component. The number of essential strings for the associated Flores component is thus $\text{g.c.d.}(P_{cF}, B^*) = \text{g.c.d.}(5, 6) = 1$.

Hence the total number of essential strings for the Flores Knot is 15, whereas the Herringbone Pineapple knot required 11 essential strings.

The Flores Knots in the above two examples are only of practical value if their greater number of essential strings, as compared to the number of essential strings in the Herringbone Pineapple Knots from which they have evolved, is used for special colour effects. Such a special colour effect is shown in Fig. 720.

Although there are for Flores Knots, evolved from A -pass Standard or Semi-Standard Herringbone Pineapple Knots, two ways to superimpose on the non-coded crossings a coding so that all those near the left bight-edge are coded identically and opposite to those near the right bight-edge, note that for $A > 2$ only a row-coding for the rows to which they belong can be achieved; the columns to which they belong cannot become column-coded. Hence the row-coded case is the general one, whereas the column-coded case is specific to $A = 2$ only. Hence of the above two ways to superimpose a coding on the non-coded crossings, let's call one the **row-coding case** and the other the **non row-coding case**.

The algorithm diagrams from which we read the half-cycle braiding algorithms for the Flores knots evolved from A -pass Standard or Semi-Standard Herringbone Pineapple Knots can be derived in the following way :

Imagine that we modify the string-run of such a Flores Knot a little further so that the string-run becomes that of a Standard or Semi-Standard Herringbone Pineapple Knot again. For the above two Examples this is shown in Fig. 721. All the components (if any) which do not have a bight-boundary 1 in the grid-diagram with this modified string-run are true components of the Flores Knot (let's call these the true Flores Knot components). Hence the grid-diagram with this modified string-run has either one component (when it has a component with the left and the right bight-boundary both 1) or two components (when one component has the left bight-boundary 1, and another component has the right bight-boundary 1) which is/are not true components of the Flores Knot (let's call this/these the nontrue Flores Knot component(s)). In practice we can then first braid the true Flores Knot components (if there are any), and finally braid the reconverted nontrue Flores Knot component(s).

The row-coding case :

In the modified Flores Knot grid-diagram a lower-left to upper-right half-cycle running from l_i to r_i has the coding sequence :

$$(l_i-1)u-(A+1-l_i)o-(l_i)u-Ao-Au-\dots-Au-Ao-(r_i-1)u-(A-r_i)o-(r_i)u,$$

in which each set of crossings, except the first set $(l_i - 1)u$ and the two penultimate sets $(r_i - 1)u - (A - r_i)o$, has one crossing belonging to string-run of the component between the bight-boundaries l_i and r_i .

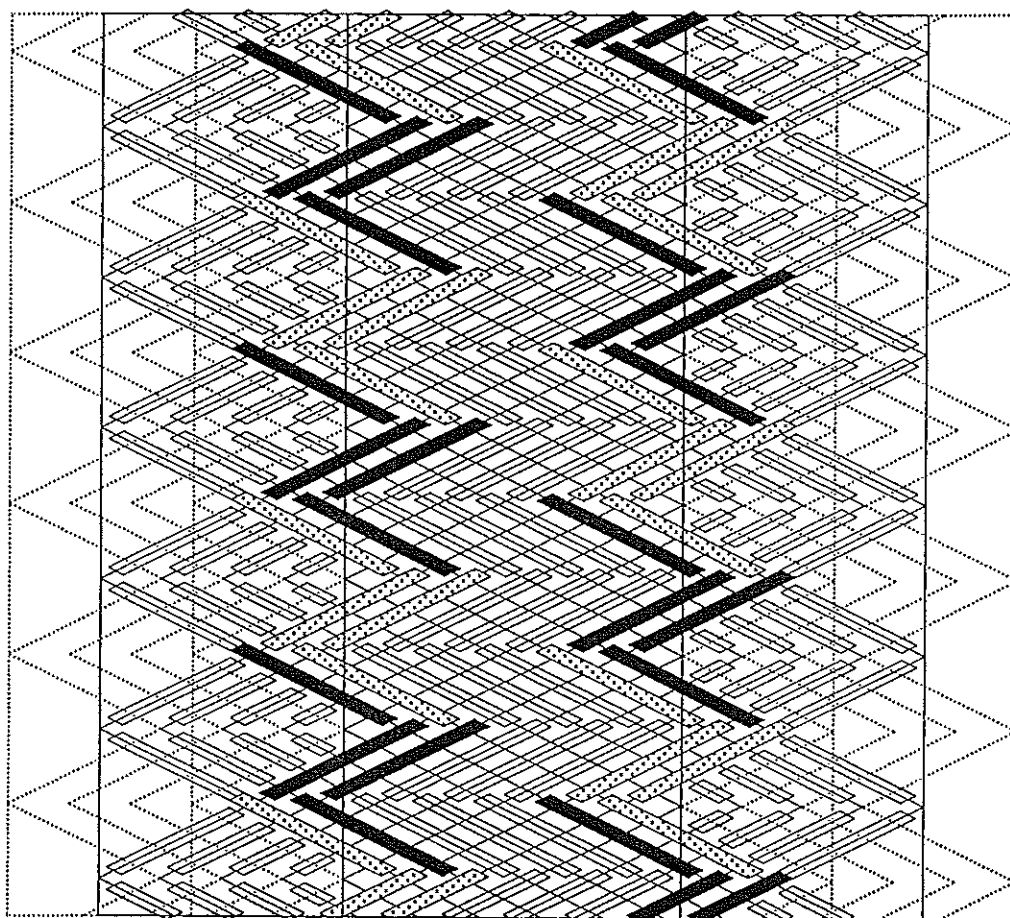
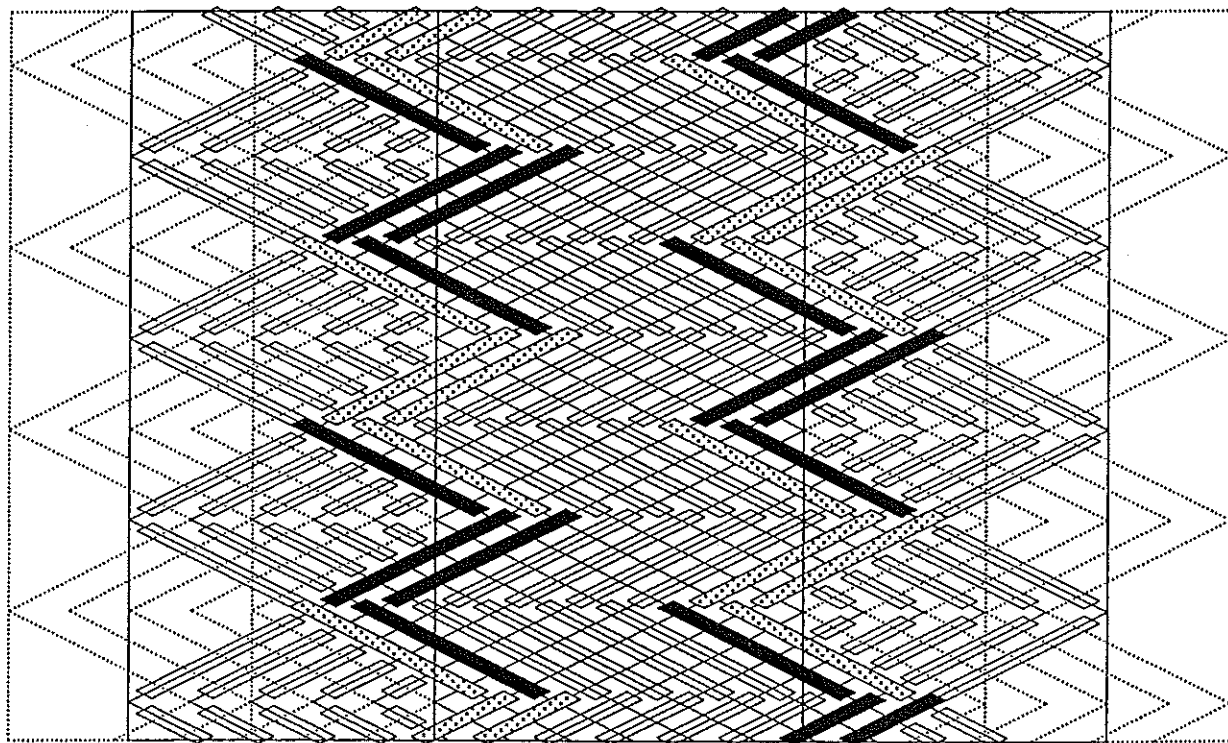


Fig. 720 — Flores Knots evolved from Standard or Semi-Standard Herringbone Pineapple Knots.

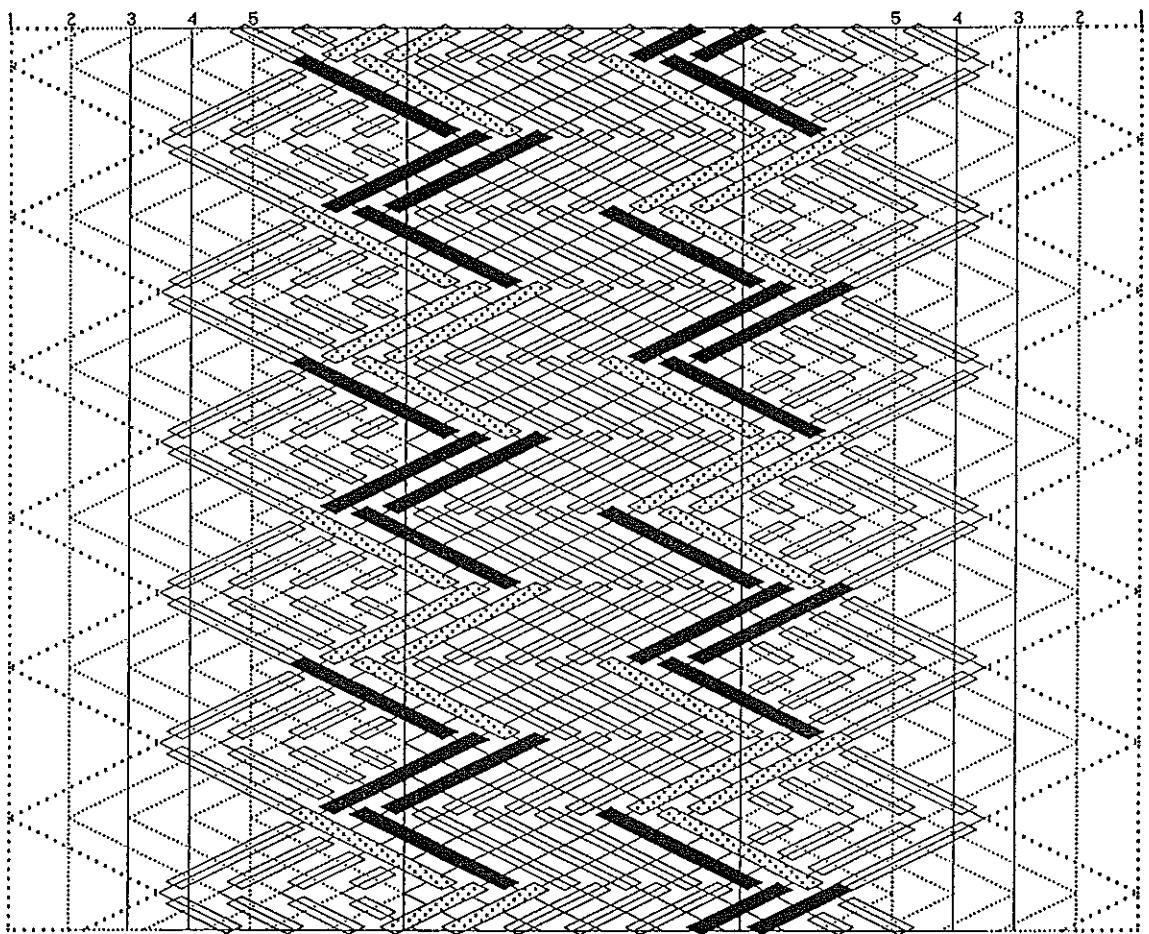
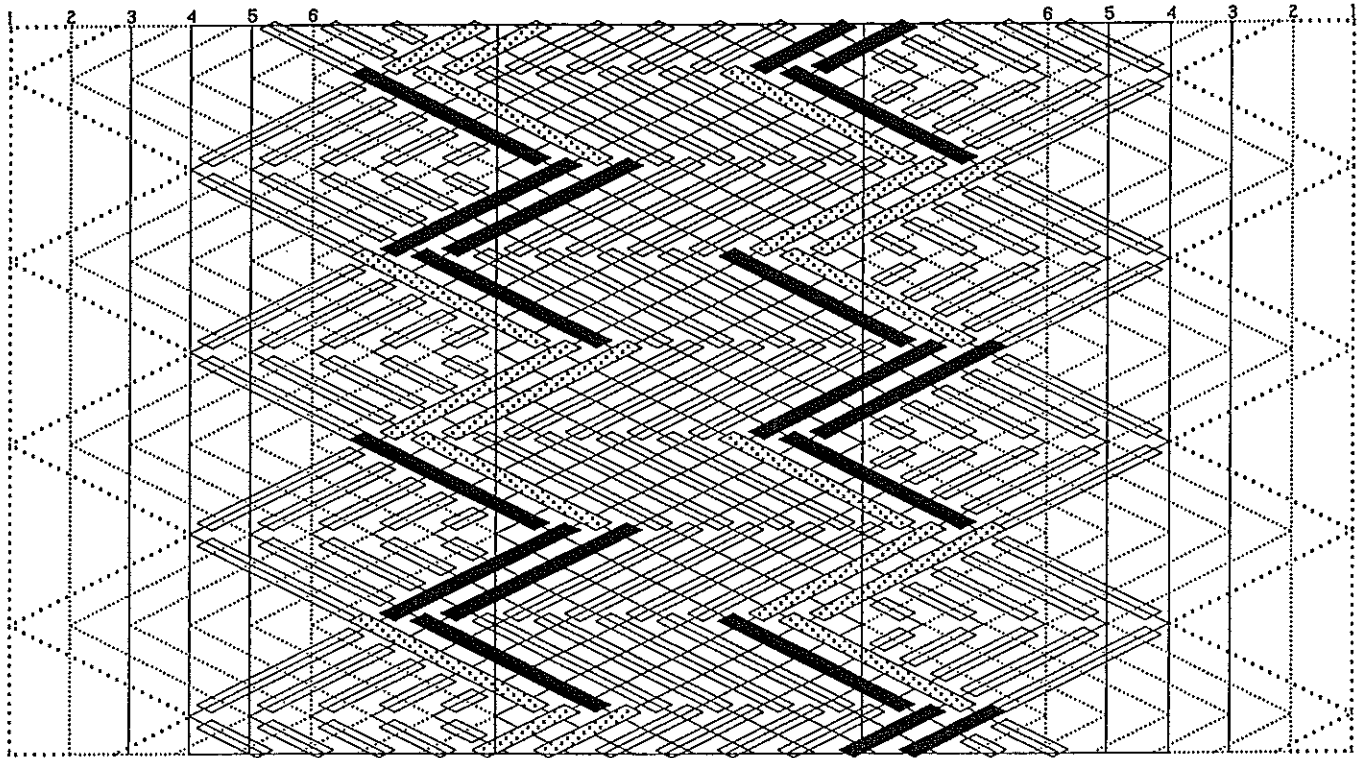


Fig. 721 — Flores Knot string-runs modified into Standard or Semi-Standard Herringbone Pineapple Knot string-runs.

In the modified Flores Knot grid-diagram a lower-right to upper-left half-cycle running from r_i to l_i has the coding sequence:

$$(r_i-1)u-(A+1-r_i)o-(r_i)u-Ao-Au-\dots-Au-Ao-(l_i-1)u-(A-l_i)o-(l_i)u,$$

in which each set of crossings, except the first set $(r_i - 1)u$ and the two penultimate sets $(l_i - 1)u - (A - l_i)o$, has one crossing belonging to the string-run of the component between the bight-boundaries l_i and r_i .

Hence the reference half-cycle sequences, consequently the first half-cycle sequences of the components, are:

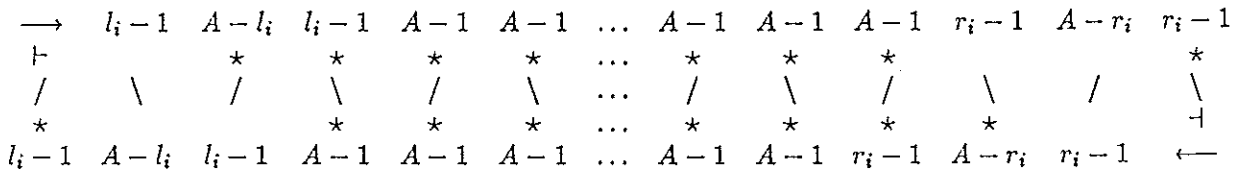
From lower-left l_i to upper-right r_i :

$$(l_i-1)u-(A-l_i)o-(l_i-1)u-(A-1)o-(A-1)u-\dots-(A-1)u-(A-1)o-(r_i-1)u-(A-r_i)o-(r_i-1)u.$$

From lower-right r_i to upper-left l_i :

$$(r_i-1)u-(A-r_i)o-(r_i-1)u-(A-1)o-(A-1)u-\dots-(A-1)u-(A-1)o-(l_i-1)u-(A-l_i)o-(l_i-1)u.$$

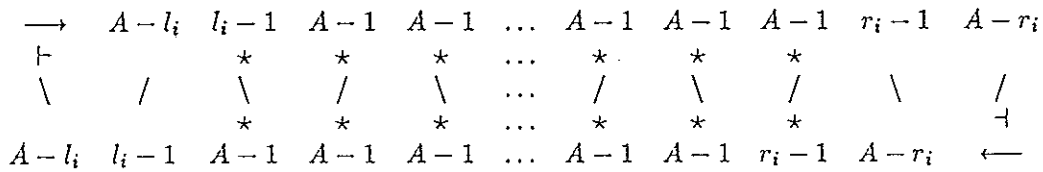
The general form of the algorithm diagram for the true Flores Knot components is thus:



The positions of the stars are occupied by the i -values of the complementary bight-number scheme associated with the component to be braided. The value above an upper star, or below a lower star, increases by 1 when its associated i -value is applicable to the half-cycle concerned. For all the lower-left to upper-right half-cycles the first entry $(l_i - 1)u$ and the last two penultimate entries $(r_i - 1)u - (A - r_i)o$ remain the same. Similarly, for all the lower-right to upper-left half-cycles the first entry $(r_i - 1)u$ and the last two penultimate entries $(l_i - 1)u - (A - l_i)o$ remain the same.

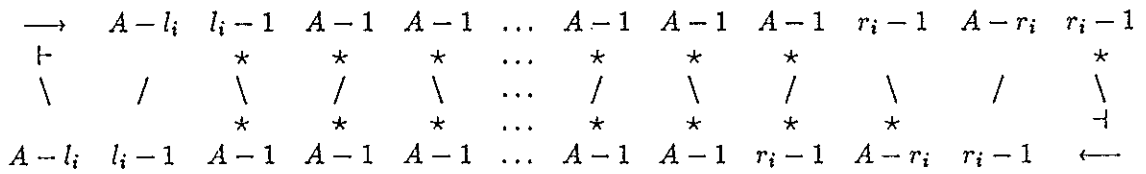
After the true Flores Knot components (if there are any) have been braided, we finally braid the reconverted nontrue Flores Knot component(s).

If there is only one nontrue Flores Knot component, then the algorithm diagram for its reconverted form (its true form) is:



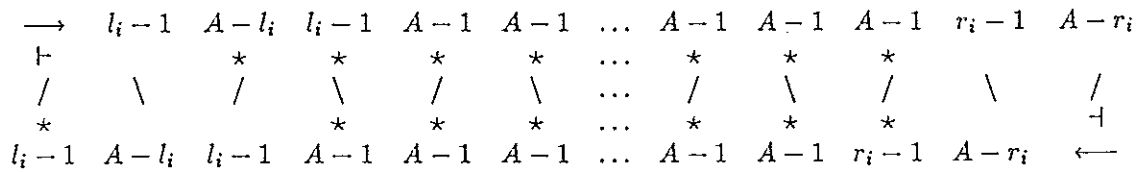
The positions of the stars are occupied by the i -values of the complementary bight-number scheme associated with the reconverted component to be braided. The value above an upper star, or below a lower star, increases by 1 when its associated i -value is applicable to the half-cycle concerned. For all the lower-left to upper-right half-cycles the first entry $(A - l_i)o$ and the last two entries $(r_i - 1)u - (A - r_i)o$ remain the same. Similarly, for all the lower-right to upper-left half-cycles the first entry $(A - r_i)o$ and the last two entries $(l_i - 1)u - (A - l_i)o$ remain the same.

If there are two nontrue Flores Knot components, then the algorithm diagram for the reconverted form (the true form) of the nontrue Flores Knot component with left bight-boundary 1 is:



The positions of the stars are occupied by the i -values of the complementary bight-number scheme associated with the reconverted component to be braided. The value above an upper star, or below a lower star, increases by 1 when its associated i -value is applicable to the half-cycle concerned. For all the lower-left to upper-right half-cycles the first entry $(A - l_i)o$ and the last two penultimate entries $(r_i - 1)u - (A - r_i)o$ remain the same. Similarly, for all the lower-right to upper-left half-cycles the first entry $(r_i - 1)u$ and the last two entries $(l_i - 1)u - (A - l_i)o$ remain the same.

The algorithm diagram for the reconverted form (the true form) of the nontrue Flores Knot component with right bight-boundary 1 is:



The positions of the stars are occupied by the i -values of the complementary bight-number scheme associated with the reconverted component to be braided. The value above an upper star, or below a lower star, increases by 1 when its associated i -value is applicable to the half-cycle concerned. For all the lower-left to upper-right half-cycles the first entry $(l_i - 1)u$ and the last two entries $(r_i - 1)u - (A - r_i)o$ remain the same. Similarly, for all the lower-right to upper-left half-cycles the first entry $(A - r_i)o$ and the last two penultimate entries $(l_i - 1)u - (A - l_i)o$ remain the same.

Example 3 :

Take the Flores Knot depicted by the upper grid-diagram in Fig. 720 under the row-coding case; $A = 6$; $B^* = 4$; $x = 24$.

Then for the string-run of a Standard or Semi-Standard Herringbone Pineapple Knot we obtain :

$$\begin{aligned}
 \text{For } l_1 = 1 \quad \longrightarrow \quad r_1 &= \left\lfloor \frac{x + A}{2} - 1 \right\rfloor_A = \left\lfloor \frac{24 + 6}{2} - 1 \right\rfloor_6 = 2 = k. \\
 n &= \frac{x + A - 2k - 2}{2A} = \frac{24 + 6 - 2 \times 2 - 2}{2 \times 6} = 2, \text{ hence :}
 \end{aligned}$$

$P_{cP} = 3 + 2n = 3 + 2 \times 2 = 7$ for $k = 2$ components. These are nontrue Flores Knot components with the half-cycles $1 \longrightarrow 2$ and $2 \longrightarrow 1$ respectively. Hence $P_{cF} = 6$ for their reconverted components.

$P'_{cP} = 1 + 2n = 1 + 2 \times 2 = 5$ for $A - k = 6 - 2 = 4$ components. These are true Flores Knot components, hence with $P'_{cF} = 5$ each.

Since $\text{g.c.d.}(P_{cF}, B^*) = \text{g.c.d.}(6, 4) = 2$, each of the two reconverted components require two essential strings. The other four components, with $\text{g.c.d.}(P'_{cF}, B^*) = \text{g.c.d.}(5, 4) = 1$, require one essential string each.

Say we braid the various components in the six sequential stages depicted in Fig. 722.

Stage 1. We first braid the component which in the upper diagram of Fig. 721 starts with the half-cycle which runs from lower-left to upper-right between left bight-boundary 3 and right bight-boundary 6. Then, at present, for this component the left bight-boundary is 1 and the right bight-boundary is 1.

Stage 2. Next we interbraid the component which in the upper diagram of Fig. 721 starts with the half-cycle which runs from lower-left to upper-right between left bight-boundary 4 and right bight-boundary 5. Then, at present, for this component the left bight-boundary is 2 and the right bight-boundary is 1.

Stage 3. Next we interbraid the component which in the upper diagram of Fig. 721 starts with the half-cycle which runs from lower-left to upper-right between left bight-boundary 5 and right bight-boundary 4. Then, at present, for this component the left bight-boundary is 3 and the right bight-boundary is 1.

Stage 4. Next we interbraid the component which in the upper diagram of Fig. 721 starts with the half-cycle which runs from lower-left to upper-right between left bight-boundary 6 and right bight-boundary 3. Then, at present, for this component the left bight-boundary is 4 and the right bight-boundary is 1.

This completes the braiding of the true Flores Knot components. Next we interbraid the two reconverted nontrue Flores Knot components.

Stage 5. The first one we interbraid runs in the upper diagram of Fig. 721 as a nontrue Flores Knot component between left bight-boundary 1 and right bight-boundary 2. Hence for this nontrue Flores Knot component, which results into two reconverted sub-components, the left bight-boundary is 1 and the right bight-boundary is 1.

Stage 6. Finally we interbraid the other reconverted nontrue Flores Knot component, which as a nontrue Flores Knot runs in the upper diagram of Fig. 721 as a nontrue Flores Knot component between left bight-boundary 2 and right bight-boundary 1. For this nontrue Flores Knot component, which results into two reconverted sub-components, the left bight-boundary is 2 and the right bight-boundary is 1.

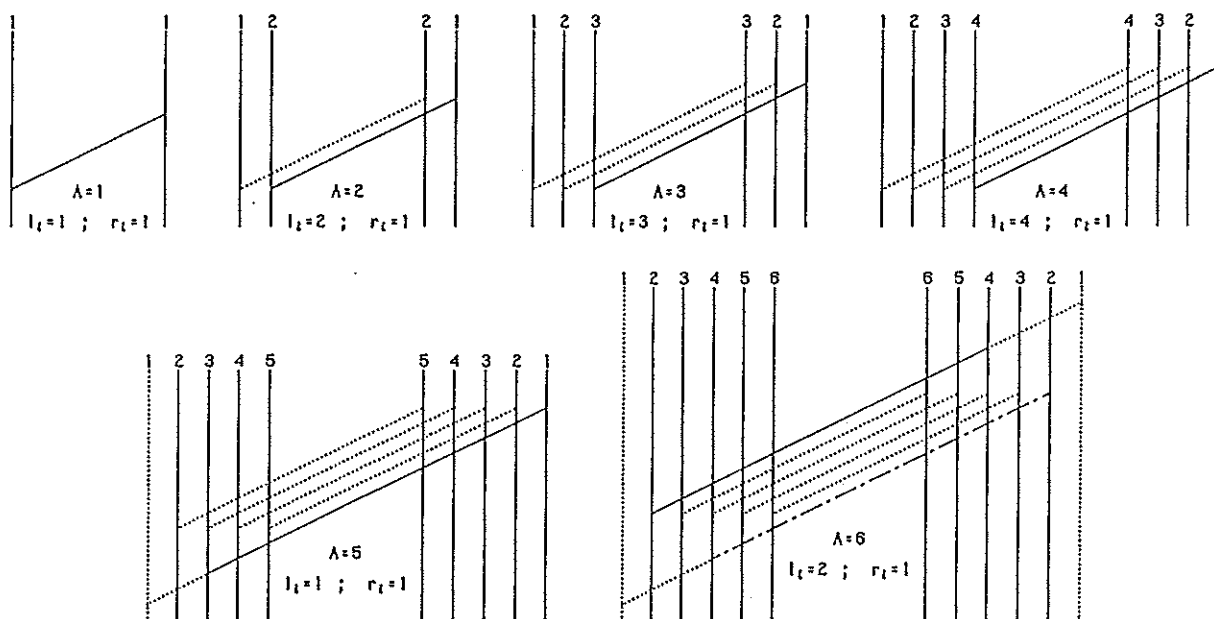
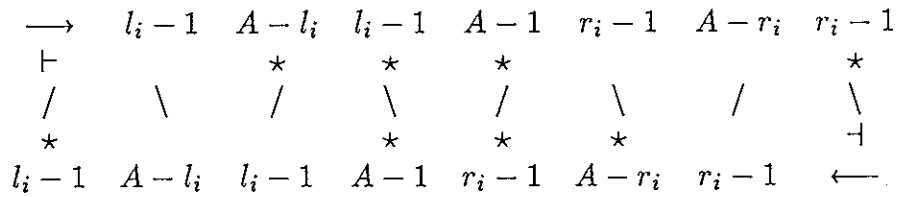


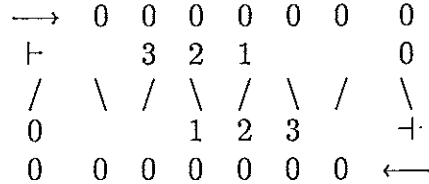
Fig. 722 — The sequence of braiding the various components.

Each of the components in the stages 1, 2, 3 and 4 require only one essential string in their construction. Each of these components is a Regular Knot with 5-parts and 4-bights, hence their Δ^* -value is equal to 3, and their generalised algorithm diagrams

are as follows:



The algorithm diagram for stage 1 is thus:



From this algorithm diagram we read the half-cycle braiding algorithms for stage 1:

- half-cycle 1 : $L_1 \longrightarrow R_1$ Free Run.
- half-cycle 2 $i = 0$: $L_1 \longleftarrow R_1$ u .
- half-cycle 3 $i = 0$: $L_1 \longrightarrow R_1$ u .
- half-cycle 4 $i \leq 1$: $L_1 \longleftarrow R_1$ $o - u$.
- half-cycle 5 $i \leq 1$: $L_1 \longrightarrow R_1$ $o - u$.
- half-cycle 6 $i \leq 2$: $L_1 \longleftarrow R_1$ $u - o - u$.
- half-cycle 7 $i \leq 2$: $L_1 \longrightarrow R_1$ $u - o - u$.
- half-cycle 8 $i \leq 3$: $L_1 \longleftarrow R_1$ $o - u - o - u$.

These half-cycle braiding steps are shown in Fig. 723.

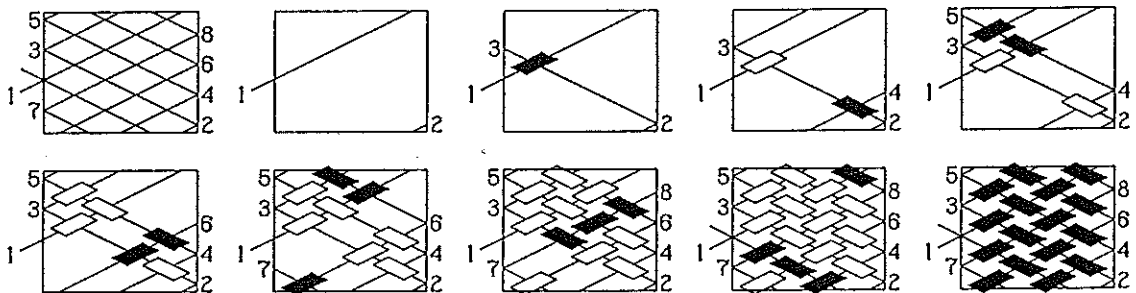
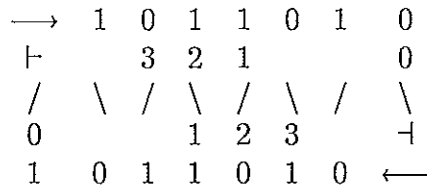


Fig. 723 — The half-cycle braiding steps for the first component.

The algorithm diagram for stage 2 is thus:



From this algorithm diagram we read the half-cycle braiding algorithms for stage 2:

- half-cycle 1 : $L_2 \longrightarrow R_1$ $2u - 2o$.
- half-cycle 2 $i = 0$: $L_2 \longleftarrow R_1$ $2o - 3u$.
- half-cycle 3 $i = 0$: $L_2 \longrightarrow R_1$ $2u - 2o - u$.
- half-cycle 4 $i \leq 1$: $L_2 \longleftarrow R_1$ $3o - 3u$.
- half-cycle 5 $i \leq 1$: $L_2 \longrightarrow R_1$ $2u - 3o - u$.
- half-cycle 6 $i \leq 2$: $L_2 \longleftarrow R_1$ $o - u - 2o - 3u$.
- half-cycle 7 $i \leq 2$: $L_2 \longrightarrow R_1$ $3u - 3o - u$.
- half-cycle 8 $i \leq 3$: $L_2 \longleftarrow R_1$ $2o - u - 2o - 3u$.

These half-cycle braiding steps are shown in Fig. 724.

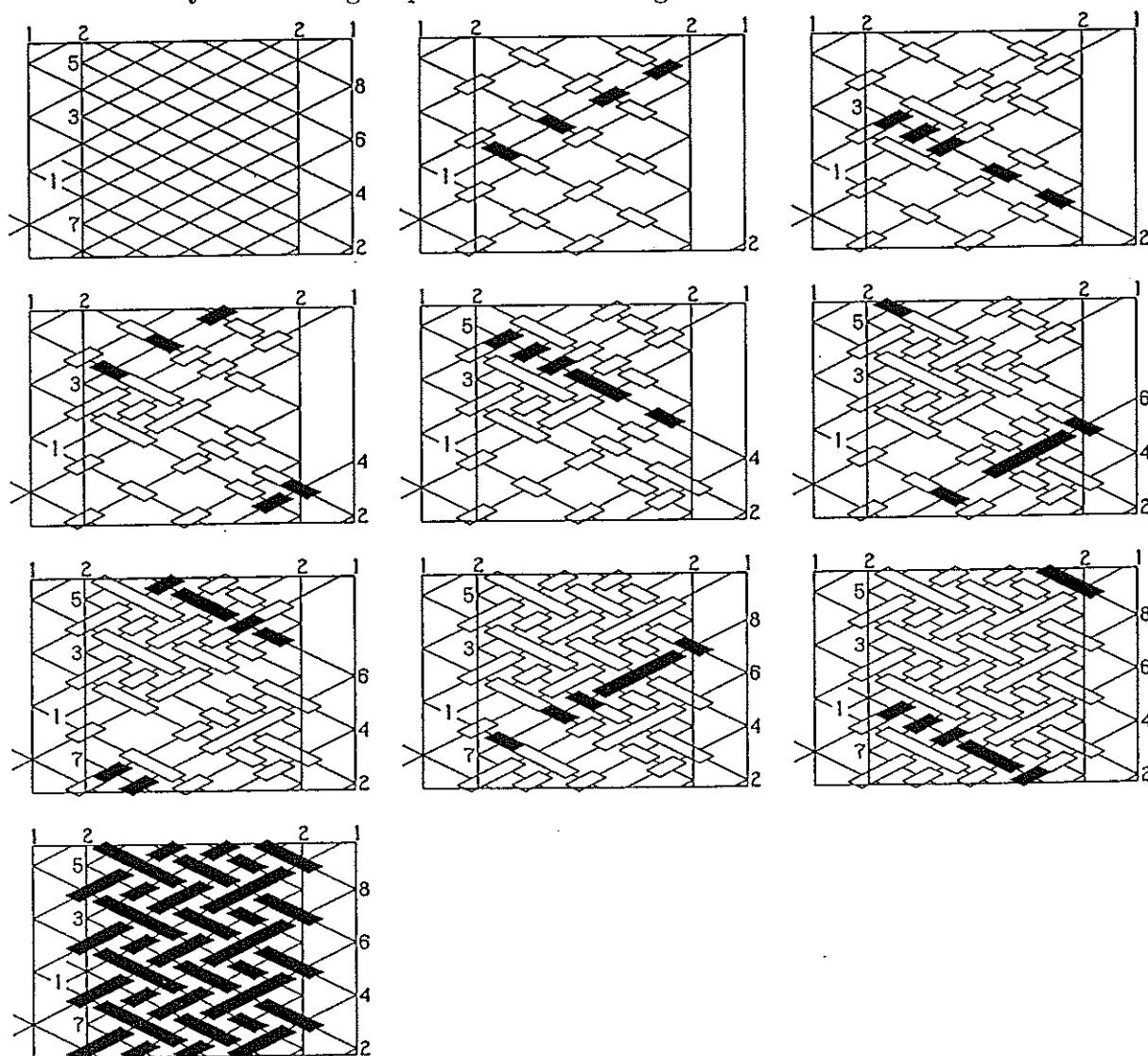
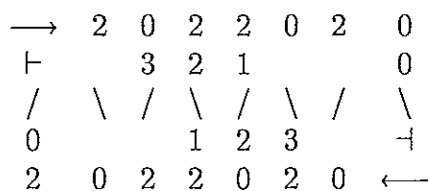


Fig. 724 — The half-cycle braiding steps for the second component.

The algorithm diagram for stage 3 is thus:



From this algorithm diagram we read the half-cycle braiding algorithms for stage 3:

- half-cycle 1 : $L_3 \rightarrow R_1$ $4u - 4o$.
- half-cycle 2 $i = 0$: $L_3 \leftarrow R_1$ $4o - 5u$.
- half-cycle 3 $i = 0$: $L_3 \rightarrow R_1$ $4u - 4o - u$.
- half-cycle 4 $i \leq 1$: $L_3 \leftarrow R_1$ $5o - 5u$.
- half-cycle 5 $i \leq 1$: $L_3 \rightarrow R_1$ $4u - 5o - u$.
- half-cycle 6 $i \leq 2$: $L_3 \leftarrow R_1$ $2o - u - 3o - 5u$.
- half-cycle 7 $i \leq 2$: $L_3 \rightarrow R_1$ $5u - 5o - u$.
- half-cycle 8 $i \leq 3$: $L_3 \leftarrow R_1$ $3o - u - 3o - 5u$.

These half-cycle braiding steps are shown in Fig. 725.

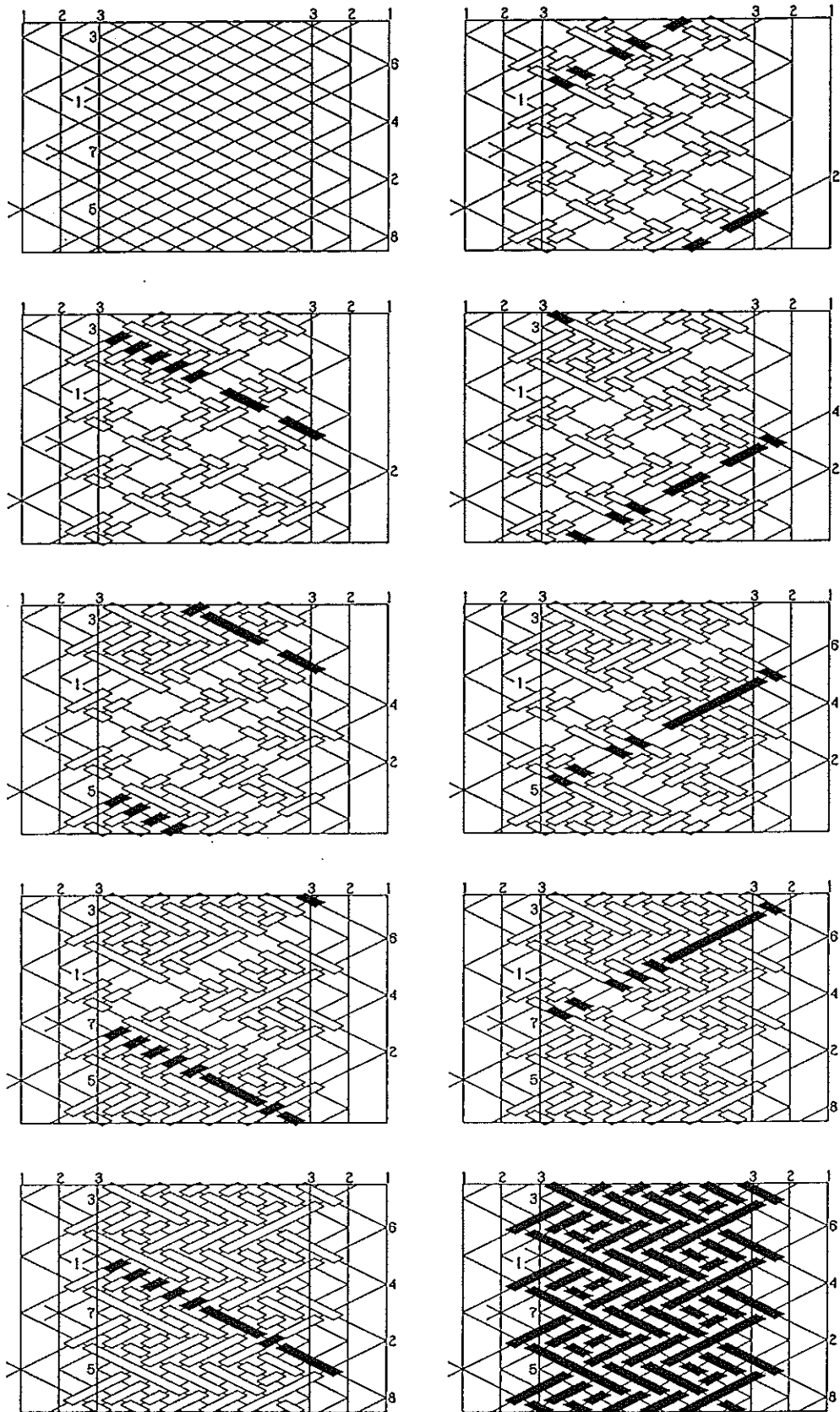
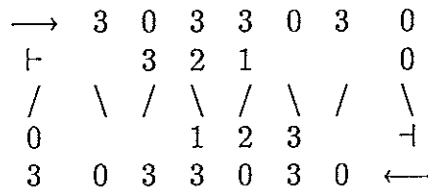


Fig. 725 — The half-cycle braiding steps for the third component.

The algorithm diagram for stage 4 is thus :



From this algorithm diagram we read the half-cycle braiding algorithms for stage 4:

- half-cycle 1 : $L_4 \longrightarrow R_1$ $6u - 6o$.
- half-cycle 2 $i = 0$: $L_4 \longleftarrow R_1$ $6o - 7u$.
- half-cycle 3 $i = 0$: $L_4 \longrightarrow R_1$ $6u - 6o - u$.
- half-cycle 4 $i \leq 1$: $L_4 \longleftarrow R_1$ $7o - 7u$.
- half-cycle 5 $i \leq 1$: $L_4 \longrightarrow R_1$ $6u - 7o - u$.
- half-cycle 6 $i \leq 2$: $L_4 \longleftarrow R_1$ $3o - u - 4o - 7u$.
- half-cycle 7 $i \leq 2$: $L_4 \longrightarrow R_1$ $7u - 7o - u$.
- half-cycle 8 $i \leq 3$: $L_4 \longleftarrow R_1$ $4o - u - 4o - 7u$.

These half-cycle braiding steps are shown in Fig. 726.

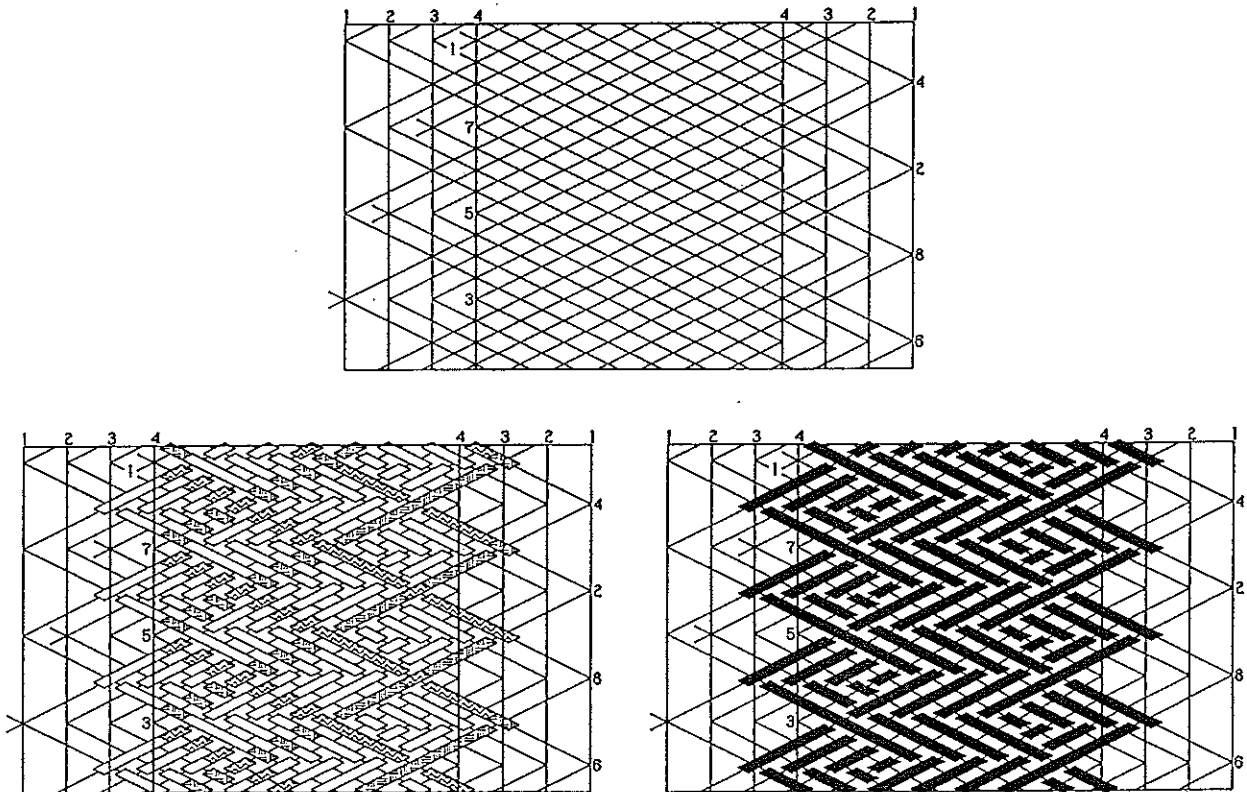
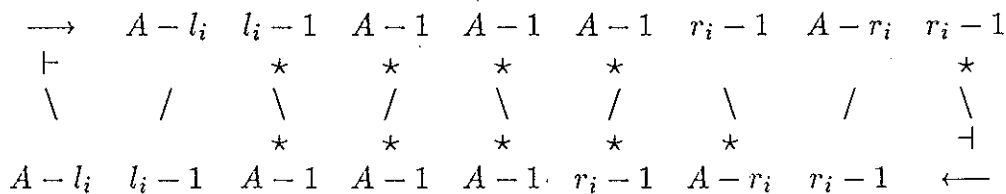
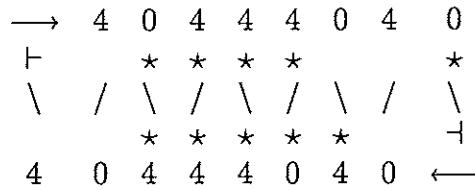


Fig. 726 — The half-cycle braiding steps for the fourth component.

The string-run of the nontrue Flores Knot component associated with stage 5 runs in Fig. 721 between left bight-boundary 1 and right bight-boundary 2. Hence the generalised algorithm diagram of the reverted component associated with stage 5 is as follows:

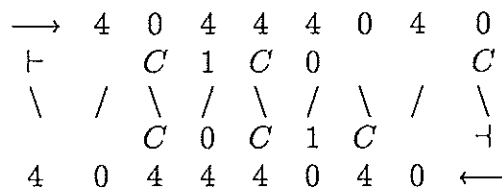


The algorithm diagram for the reconverted component associated with stage 5 is thus:

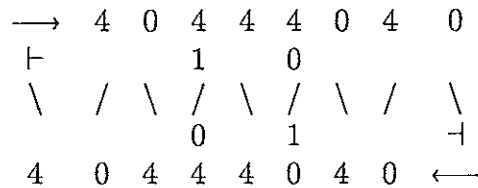


The reconverted component associated with braiding stage 5 has 6-parts and 4-bights, and since $\text{g.c.d.}(6, 4) = 2$, it requires two essential strings in its construction; hence the reconverted component consists of two sub-components. Each sub-component is a Regular Knot with 3-parts and 2-bights, hence its Δ^* -value is 1.

Since this reconverted component consists of two sub-components, the i -values for the stars are as shown in the reconverted component's algorithm diagram below:



This algorithm diagram gives us the following algorithm diagram for the first to be braided sub-component:

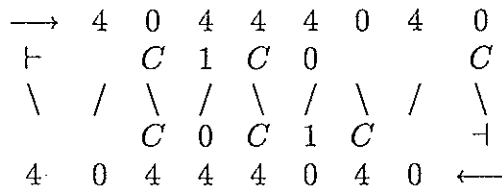


From this algorithm diagram we read the half-cycle braiding algorithms for the first to be braided sub-component associated with stage 5:

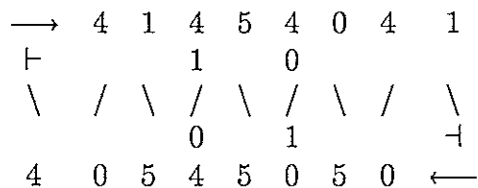
- half-cycle 1 : $L \longrightarrow R_1 \quad 8o - 4u - 8o.$
- half-cycle 2 $i = 0$: $L \longleftarrow R_1 \quad 8o - 5u - 8o.$
- half-cycle 3 $i = 0$: $L \longrightarrow R_1 \quad 8o - 4u - 9o.$
- half-cycle 4 $i \leq 1$: $L \longleftarrow R_1 \quad 4o - u - 4o - 5u - 8o.$

These half-cycle braiding steps are shown in the upper diagram of Fig. 727.

From the algorithm diagram



we obtain the following algorithm diagram for the next to be braided sub-component associated with stage 5:

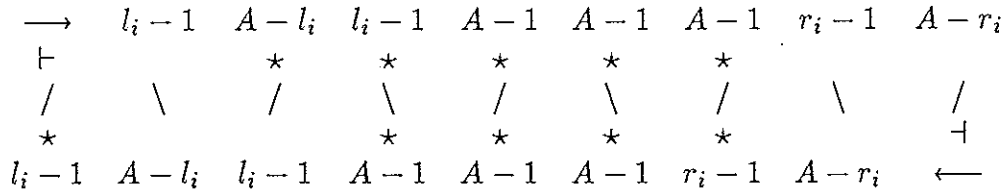


From this algorithm diagram we read the following half-cycle braiding algorithms for the second sub-component associated with stage 5:

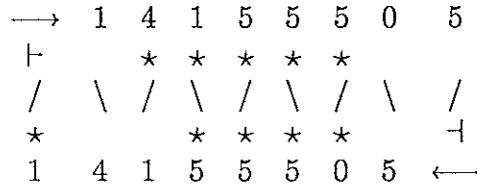
half-cycle 1	:	$L \longrightarrow R_1$	$4o - u - 4o - 5u - 8o - u.$
half-cycle 2	$i = 0$	$L \longleftarrow R_1$	$10o - 5u - 9o.$
half-cycle 3	$i = 0$	$L \longrightarrow R_1$	$4o - u - 4o - 5u - 9o - u.$
half-cycle 4	$i \leq 1$	$L \longleftarrow R_1$	$5o - u - 5o - 5u - 9o.$

These half-cycle braiding steps are shown in the central diagram of Fig. 727.

The string-run of the nontrue Flores Knot component associated with stage 6 runs in Fig. 721 between left bight-boundary 2 and right bight-boundary 1. Hence the generalised algorithm diagram of the reconverted component associated with stage 6 is as follows:

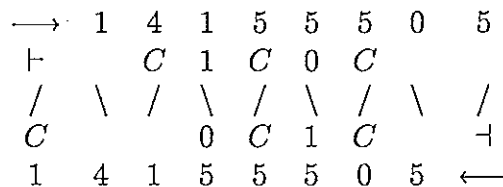


The algorithm diagram for the reconverted component associated with stage 6 is thus:

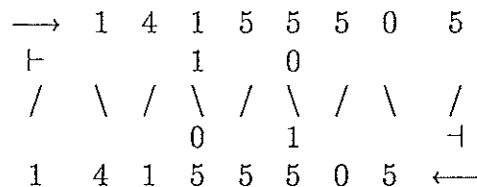


The reconverted component associated with braiding stage 6 has 6-parts and 4-bights, and since $\text{g.c.d.}(6, 4) = 2$, it requires two essential strings in its construction; hence the reconverted component consists of two sub-components. Each sub-component is a Regular Knot with 3-parts and 2-bights, hence its Δ^* -value is 1.

Since this reconverted component consists of two sub-components, the i -values for the stars are as shown in the reconverted component's algorithm diagram below:



This algorithm diagram gives us the following algorithm diagram for the first to be braided sub-component:



From this algorithm diagram we read the half-cycle braiding algorithms for the first to be braided sub-component associated with stage 6:

half-cycle 1	:	$L_2 \longrightarrow R$	$u - 4o - u - 5o - 5u - 10o.$
half-cycle 2	$i = 0$	$L_2 \longleftarrow R$	$10o - 5u - 6o - u - 4o - u.$
half-cycle 3	$i = 0$	$L_2 \longrightarrow R$	$u - 4o - u - 5o - 6u - 10o.$
half-cycle 4	$i \leq 1$	$L_2 \longleftarrow R$	$11o - 5u - 6o - u - 4o - u.$

These half-cycle braiding steps are shown in the upper diagram of Fig. 728.

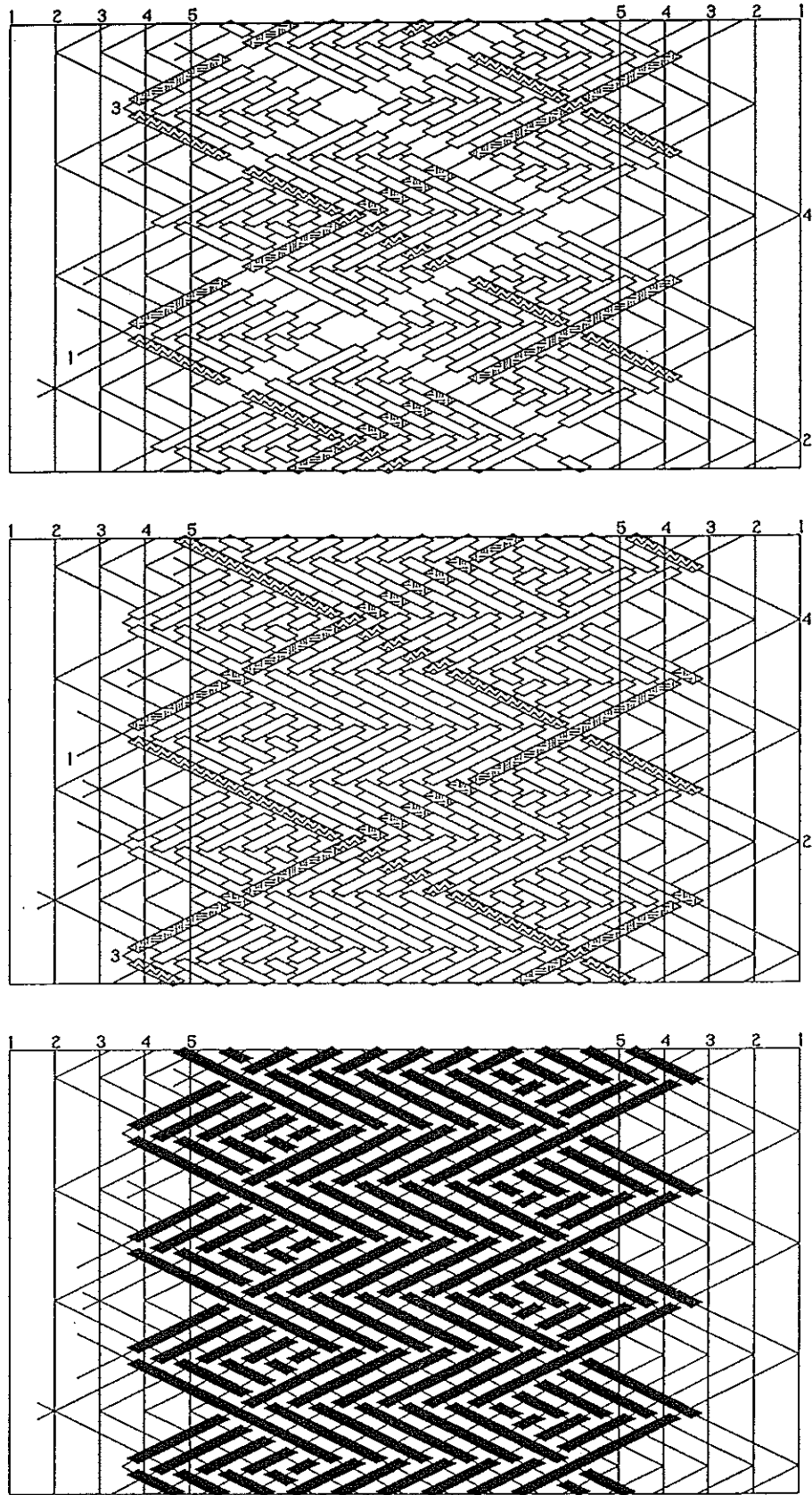


Fig. 727 — Braiding of stage 5.

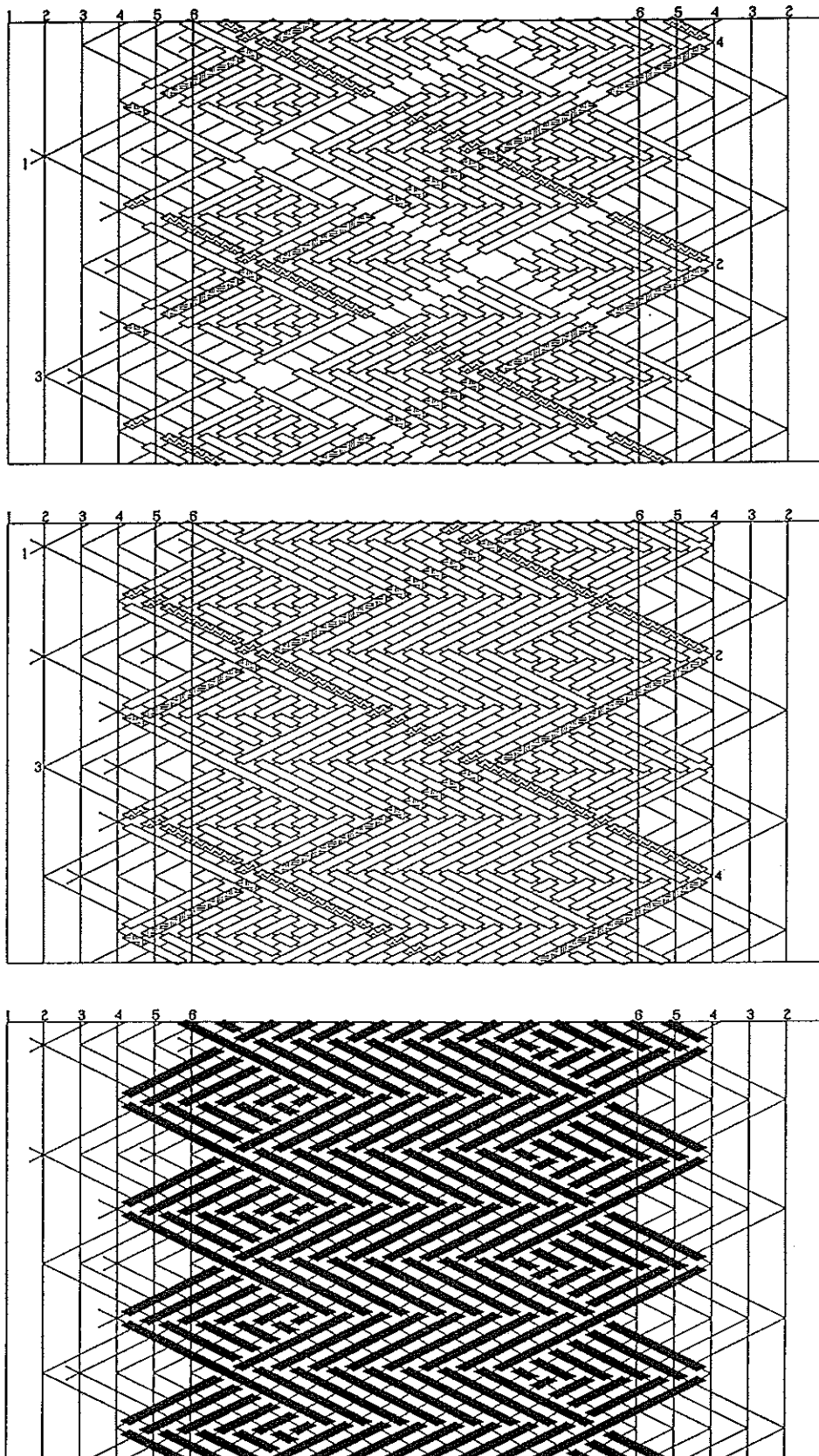
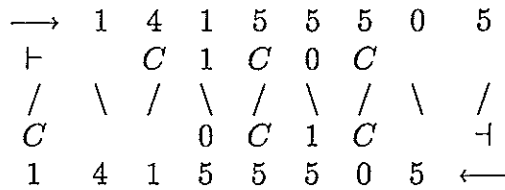
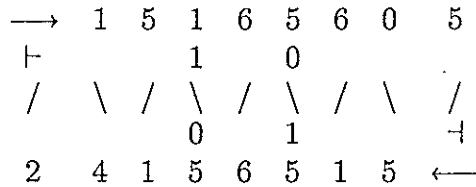


Fig. 728 — Braiding of stage 6.

From the algorithm diagram



we obtain the following algorithm diagram for the next to be braided sub-component associated with stage 6:



From this algorithm diagram we read the following half-cycle braiding algorithms for the second sub-component associated with stage 6:

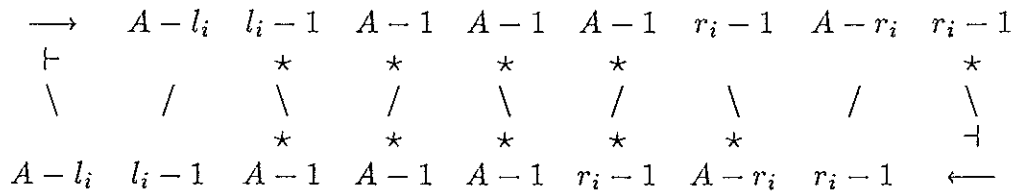
- half-cycle 1 : $L_2 \longrightarrow R \quad u - 5o - u - 6o - 5u - 11o.$
- half-cycle 2 $i = 0$: $L_2 \longleftarrow R \quad 5o - u - 5o - 6u - 6o - u - 4o - 2u.$
- half-cycle 3 $i = 0$: $L_2 \longrightarrow R \quad u - 5o - u - 6o - 6u - 11o.$
- half-cycle 4 $i \leq 1$: $L_2 \longleftarrow R \quad 5o - u - 6o - 6u - 6o - u - 4o - 2u.$

These half-cycle braiding steps are shown in the central diagram of Fig. 728.

Note that the components of this Flores knot can of course be braided in several different sequences, similar to braiding the components of Standard and Semi-Standard Herrinbone Pineapple Knots[†].

$A = 5$; $B^* = 6$; $x = 21$ for the Flores Knot depicted by the lower grid-diagram in Fig. 720, with $P'_{cF} = 5$ for each of the three true Flores Knot components and $P_{cF} = 6$ for the two reconverted nontrue Flores Knot components. First we braid again the three true Flores Knot components and finally the two reconverted nontrue Flores Knot components. Each of the two reconverted nontrue Flores Knot components requires six essential strings since $\text{g.c.d.}(P_{cF}, B^*) = \text{g.c.d.}(6, 6) = 6$. Say that after we have braided the three true Flores Knot components we first braid the reconverted nontrue Flores Knot component of the nontrue Flores Knot component which runs between left bight-boundary 1 and right bight-boundary 2 in Fig. 729. For the braiding of this component $A = 4$; $l_i = 1$; $r_i = 1$. Say that we braid its six sub-components in the sequence shown in Fig. 729. Since each sub-component has 1-part and 1-bight, the Δ^* -value of each sub-component is equal to 0.

The generalised algorithm diagram of the reconverted component is as follows:



The algorithm diagram for the reconverted component is thus:

[†] Refer to *The Braider*, Issue No. 23.

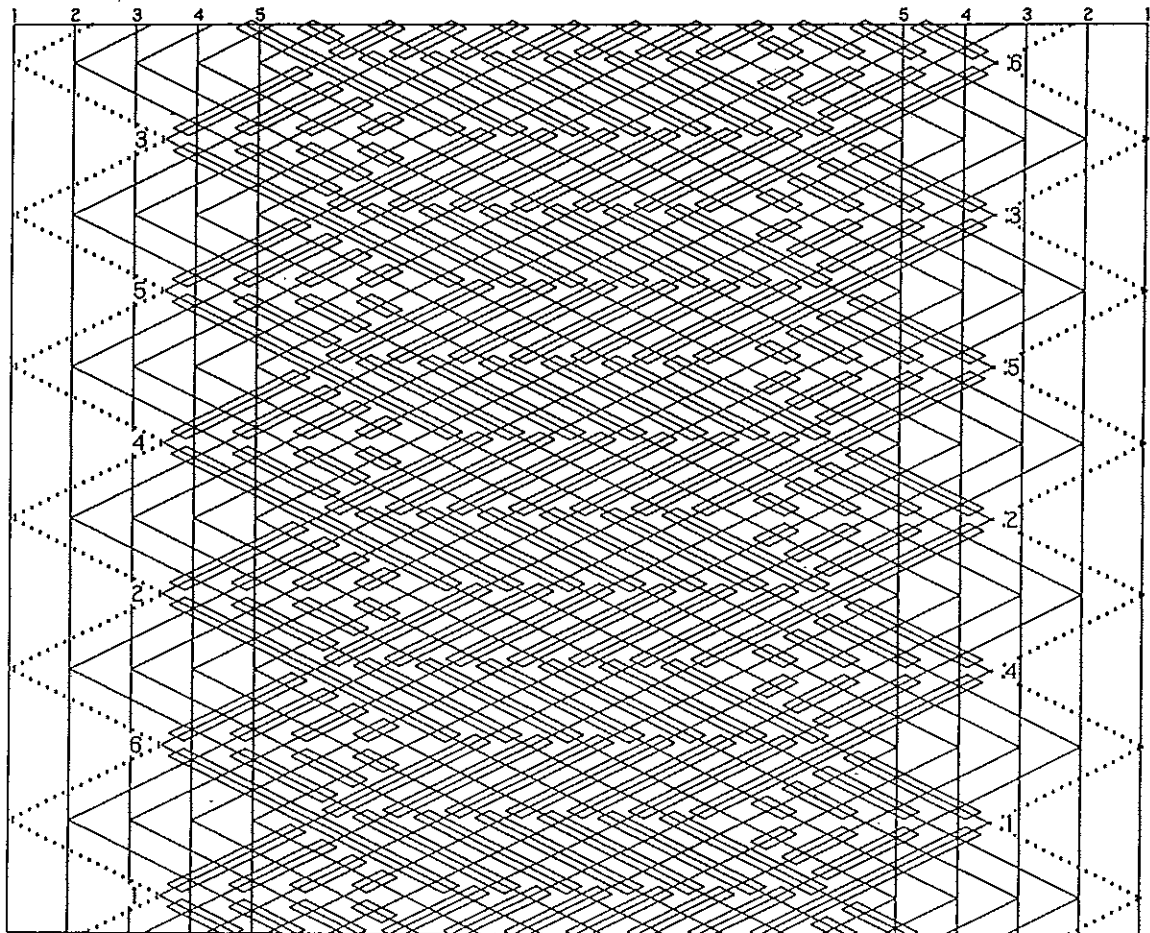
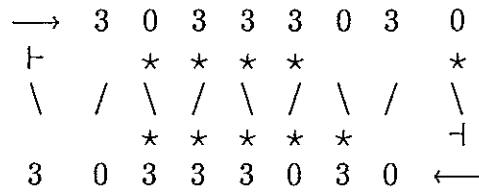
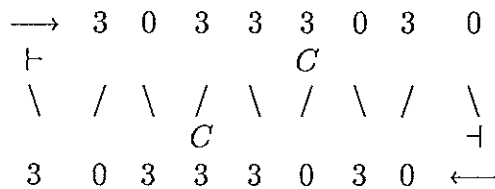
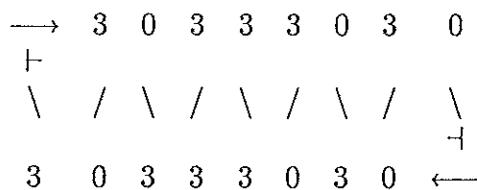


Fig. 729 — A Flores Knot with $A = 5$; $B^* = 6$; $x = 21$.

For sub-components 1 and 2 the algorithm diagram is:



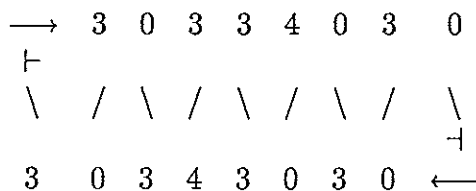
Hence for sub-component 1 the algorithm diagram is:



From this algorithm diagram we read the following half-cycle braiding algorithms for this sub-component:

$$\begin{aligned} \text{half-cycle 1} & : L \longrightarrow R_1 & 6o - 3u - 6o. \\ \text{half-cycle 2} \quad i = 0 & : L \longleftarrow R_1 & 6o - 3u - 6o. \end{aligned}$$

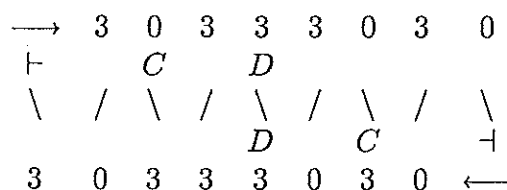
Hence for sub-component 2 the algorithm diagram is:



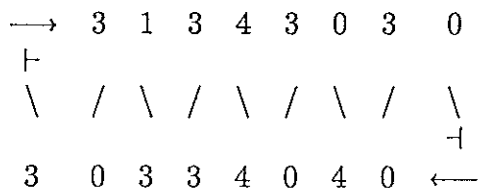
From this algorithm diagram we read the following half-cycle braiding algorithms for this sub-component:

$$\begin{aligned} \text{half-cycle 1} & : L \longrightarrow R_1 & 6o - 3u - 7o. \\ \text{half-cycle 2} \quad i = 0 & : L \longleftarrow R_1 & 6o - 4u - 6o. \end{aligned}$$

For sub-component 3 the algorithm diagram is:



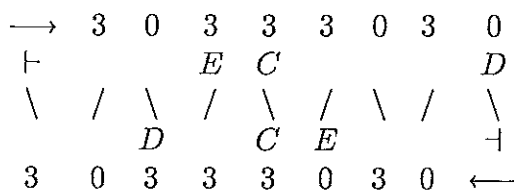
Hence for sub-component 3 the algorithm diagram is:



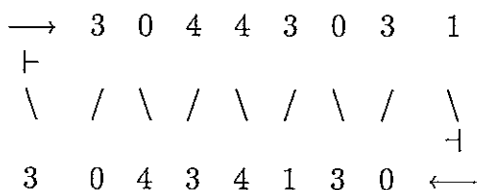
From this algorithm diagram we read the following half-cycle braiding algorithms for this sub-component:

$$\begin{aligned} \text{half-cycle 1} & : L \longrightarrow R_1 & 3o - u - 3o - 4u - 6o. \\ \text{half-cycle 2} \quad i = 0 & : L \longleftarrow R_1 & 8o - 3u - 6o. \end{aligned}$$

For sub-component 4 the algorithm diagram is:



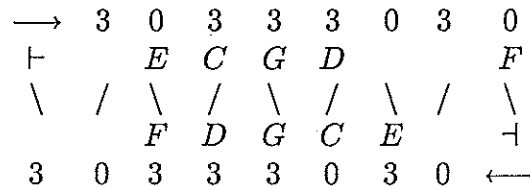
Hence for sub-component 4 the algorithm diagram is:



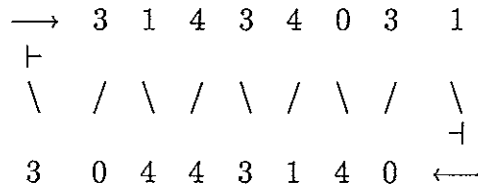
From this algorithm diagram we read the following half-cycle braiding algorithms for this sub-component:

$$\begin{aligned} \text{half-cycle 1} & : L \longrightarrow R_1 & 7o - 4u - 6o - u. \\ \text{half-cycle 2} \quad i = 0 & : L \longleftarrow R_1 & 3o - u - 4o - 3u - 7o. \end{aligned}$$

For sub-components 5 and 6 the algorithm diagram is:



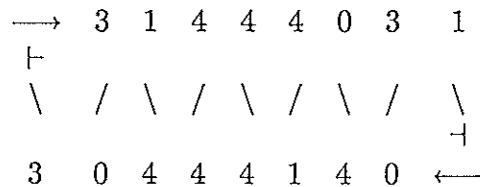
Hence for sub-component 5 the algorithm diagram is:



From this algorithm diagram we read the following half-cycle braiding algorithms for this sub-component:

$$\begin{array}{ll}
 \text{half-cycle 1} & : \quad L \longrightarrow R_1 \quad 3o - u - 4o - 3u - 7o - u. \\
 \text{half-cycle 2} \quad i = 0 & : \quad L \longleftarrow R_1 \quad 4o - u - 3o - 4u - 7o.
 \end{array}$$

Hence for sub-component 6 the algorithm diagram is:



From this algorithm diagram we read the following half-cycle braiding algorithms for this sub-component:

$$\begin{array}{ll}
 \text{half-cycle 1} & : \quad L \longrightarrow R_1 \quad 3o - u - 4o - 4u - 7o - u. \\
 \text{half-cycle 2} \quad i = 0 & : \quad L \longleftarrow R_1 \quad 4o - u - 4o - 4u - 7o.
 \end{array}$$

In practice we wouldn't of course braid in the above sequence the six sub-components of this reconverted nontrue Flores Knot; we only took this non regular periodic sequence of construction to show the associated algorithm diagrams. Refer also to *The Braider*, Issue No. 8, pp.173-176.

★★ Say we finally braid the reconverted nontrue Flores Knot component of the nontrue Flores Knot component which runs between left bight-boundary 2 and right bight-boundary 1 in Fig. 729. Furthermore, say that we braid its six sub-components in the sequence shown in Fig. 729. Give the algorithm diagrams required and their associated half-cycle braiding algorithms.

All the Flores Knots discussed here require more than one essential string and there is no real justification at all to imitate any of them by a single string construction form. If a single string braid is desired then a Flores Knot which requires only one essential string should be employed. Such Flores Knots we shall discuss in the next issue of *The Braider*.

We also like to stress that, contrary to what Bruce Grant states on pg.424 in the *Encyclopedia of Rawhide and Leather Braiding* (see pg.903 at the beginning of our discussion concerning the Flores Knots), the Flores Knots do not have a herringbone weave.

